

Dust observations at orbital altitudes surrounding Mars

L. Andersson,¹ T. D. Weber,¹ D. Malaspina,¹ F. Cray,¹ R. E. Ergun,¹ G. T. Delory,² C. M. Fowler,¹ M. W. Morooka,¹ T. McEnulty,¹ A. I. Eriksson,³ D. J. Andrews,³ M. Horanyi,¹ A. Collette,¹ R. Yelle,⁴ B. M. Jakosky¹

Dust is common close to the martian surface, but no known process can lift appreciable concentrations of particles to altitudes above ~150 kilometers. We present observations of dust at altitudes ranging from 150 to above 1000 kilometers by the Langmuir Probe and Wave instrument on the Mars Atmosphere and Volatile Evolution spacecraft. Based on its distribution, we interpret this dust to be interplanetary in origin. A comparison with laboratory measurements indicates that the dust grain size ranges from 1 to 12 micrometers, assuming a typical grain velocity of ~18 kilometers per second. These direct observations of dust entering the martian atmosphere improve our understanding of the sources, sinks, and transport of interplanetary dust throughout the inner solar system and the associated impacts on Mars's atmosphere.

Dust in the martian atmosphere arises from several sources. Dust from the surface can be lifted to altitudes of 80 to 100 km by dust devils and during global dust storms (1), but aerosols and dust from the lower atmosphere are not expected to reach altitudes of ~200 km. Dust originating from the two moons Phobos and Deimos could reach these altitudes (2); such dust would be created by surface erosion and could create a dust ring around Mars. A dust ring would be expected to have a decreasing abundance of dust grains at low altitudes, because individual grains at these altitudes should have elliptical orbits and would be lost as a result of atmospheric friction (3). Another possible source of dust at low altitudes is interplanetary dust. These dust particles are known to enter planetary atmospheres with above-Keplerian speeds and, through ablation processes, are the primary contributor to the metallic meteor layer at around 80 km above Earth (4, 5). Thus far, interplanetary dust influx into an atmosphere has been observed only at Earth.

The Mars Atmosphere and Volatile Evolution (MAVEN) mission (6) arrived at Mars in the fall of 2014. Dust can be detected by MAVEN's Langmuir Probe and Waves (LPW) instrument owing to its ability to measure high-frequency electric fields (7). It can observe the current pulses due to plasma clouds forming when grains hit the spacecraft at orbital speeds (typically a few to a few tens of kilometers per second) and the associated changes in the spacecraft potential. Because the entire spacecraft surface acts as a detector, very low dust fluxes can be recorded. To observe these effects with an

electric field instrument, it is best to measure the potential between the sensor and the spacecraft at a high cadence (8). LPW takes snapshots of time series called data bursts (9), and the signature of a dust impact in the time series can vary (Fig. 1). The dust observed by LPW is small (nano- to micrometer grain radii), and these impacts do not endanger the spacecraft.

Dust detection using electric field instruments has been demonstrated by many previous interplanetary and planetary missions (10–15). Instrument response to a dust impact depends on many factors, including spacecraft orientation, electrical connection between spacecraft surfaces, and the design of the electric field instrument. Recently, laboratory experiments have verified that dust impacts can create signals from charge recollection on spacecraft surfaces and on the sensor itself (16). The combination of currents being collected by the spacecraft body and the antenna gives rise to a

bipolar voltage signature (Fig. 1, top). The current collected from the plasma cloud can be positive or negative, depending on the surface potential with respect to the plasma potential. At low altitudes, MAVEN charges negatively and therefore is collecting ion currents from the plasma cloud.

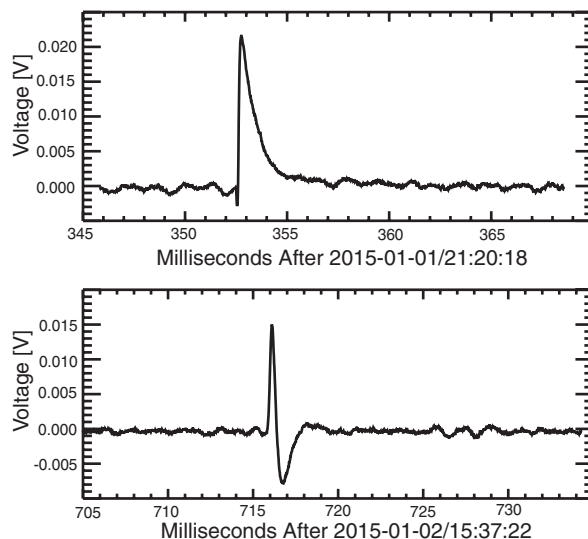
The LPW instrument only intermittently records data bursts that are suitable for dust detection, and therefore only a lower bound on the observed dust fluxes can be estimated. We determined the observed flux level over ~7 months as a function of altitude (Fig. 2C). This flux is derived using the total number of measured dust impacts at each altitude and the total time the satellite spent at each altitude interval. The observed fluxes are approximately constant at high altitudes and then increase below 300 km. However, this increase at lower altitudes is probably an observational artifact, due to increased measurement sensitivity resulting from spacecraft charging (9). The fraction of bursts containing a dust signal does not vary as a function of altitude when only low charging events are included (Fig. 3).

The size of the observed dust grains can be estimated using the impact signal amplitude, after making necessary assumptions regarding the impact speed and the spacecraft material that is receiving the impacts. Recent laboratory experiments have demonstrated that many spacecraft materials have similar responses to dust impacts (17), with the amplitude of the measured voltage spike scaling predictably based on the impactor's mass and velocity. Using the same laboratory test setup, the primary surface material of the MAVEN spacecraft (a multilayer insulation) was tested, revealing the following relationship

$$Q/m = 0.0230 v^{3.42} \text{ for } v > \sim 4 \text{ km s}^{-1}$$

where v is the dust impact velocity (km s^{-1}) and Q/m is the ratio of the charge Q , liberated by the impact, to the dust grain's mass m (C kg^{-1}). This empirically determined sensitivity suggests that the MAVEN spacecraft should be able to observe

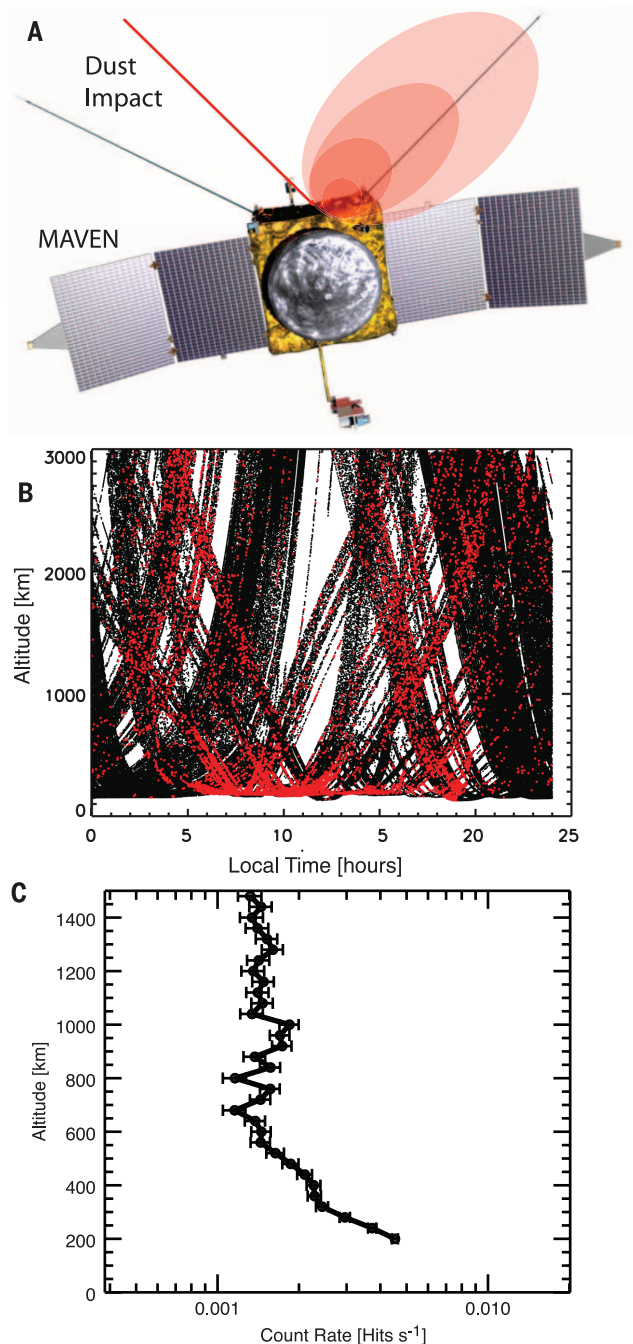
Fig. 1. Two examples of dust impacts recorded by the LPW instrument. The shape of the time series depends on the location of the impact, dust size, dust velocity, and spacecraft-to-sensor potential. **(Top)** An example of current recollection by the LPW sensor. **(Bottom)** A bipolar signal of current recollection by both the LPW sensor and the spacecraft body (16).



¹Laboratory for Atmospheric and Space Physics, University of Colorado–Boulder, Boulder, CO 80303, USA. ²Space Science Laboratory, University of California–Berkeley, Berkeley, CA 94720, USA. ³Swedish Institute of Space Physics, Uppsala, Sweden. ⁴Lunar and Planetary Laboratory, University of Arizona, Tucson, AZ 85721, USA.
*Corresponding author. E-mail: laila.andersson@lasp.colorado.edu

Fig. 2. Dust impacts on the MAVEN spacecraft observed below 1500 km.

A dust impact hitting the spacecraft is illustrated in (A). The orbit coverage from the first ~7 months of operation is shown by the black dots in (B) as function of solar zenith angle and altitude. The red dots indicate where dust impacts were observed. The lower limit on the dust count rate, as function of altitude, is shown in (C). The presented uncertainty is the standard deviation.



dust signals more frequently than other missions, such as the Solar Terrestrial Relations Observatory (17).

Dust grains are typically assumed to have a mass density of $\sim 2.5 \text{ g cm}^{-3}$ (5). The size of the dust grains can be estimated using the above relationship, the observed signal amplitude, an assumed mass density and impact velocity, and a body capacitance for the MAVEN spacecraft of $\sim 200 \text{ pF}$ (the vacuum capacity of a 2-m sphere to infinity). The observed dust-pulse amplitudes increase with decreasing altitude (Fig. 4). The dust size is derived on the basis of two assumed impact velocities: (i) the spacecraft velocity, which is $\sim 4 \text{ km/s}$,

and (ii) the expected average speed of interplanetary dust at Mars, $\sim 18 \text{ km/s}$ (18). Based on the lower bound, typical dust sizes are ~ 5 to $25 \mu\text{m}$, with a mass of $\sim 10^{-12}$ to 10^{-10} kg . Using the upper bound suggests slightly smaller grains, with sizes of ~ 1 to $5 \mu\text{m}$ and masses of $\sim 10^{-14}$ to 10^{-12} kg .

Given the observed constant or increased flux with decreasing altitude (Fig. 2C), the most likely source of the dust particles is the atmosphere. Recent imaging of Mars (19) suggests that dust may be lofted to high altitudes from the lower atmosphere. However, no currently acting physical processes are thought to be able to lift ~ 1 - to $20\text{-}\mu\text{m}$ particles to altitudes of $\sim 200 \text{ km}$ above Mars's

surface. Therefore, we conclude that the lower atmosphere is probably not the source of the observed dust.

Based on theoretical studies that model dust from Phobos and Deimos, observable densities of dust grains with masses of $\sim 10^{-12} \text{ kg}$ could be possible at altitudes below 600 km . (3). The theoretical expectations of dust fluxes at low altitudes for these masses are similar to our observed fluxes (Fig. 2C), suggesting that Phobos and Deimos could be viable sources. However, dust from the moons should be confined mainly to their respective orbital planes, resulting in a doughnut-shaped ring around the equator of Mars (3). The dust impacts observed over our ~ 7 -month period of analysis do not exhibit this shape (fig. S1), indicating that the moons are not the source of the observed dust. The dust flux from the moons is also predicted to decrease with altitude as a result of increasing gas drag and elliptical dust orbits, an effect which is not evident in our observations.

The expected interplanetary dust fluxes at 1 astronomical unit for particles of $\sim 10^{-14}$ to 10^{-12} kg are $\sim 5 \times 10^{-7}$ to $5 \times 10^{-5} \text{ m}^{-2} \text{ s}^{-1}$ (20). To compare this with the observed MAVEN fluxes, we first needed to identify the detection cross section. We assumed the upper limit of the cross section for detecting the dust to be the spacecraft body, at $\sim 9 \text{ m}^2$. Scaling the interplanetary fluxes to Mars's orbit (20), the MAVEN lower-bound dust levels are slightly higher than but close to the expected interplanetary dust fluxes, with fluxes of 10^{-4} to $5 \times 10^{-4} \text{ m}^{-2} \text{ s}^{-1}$. The atmospheric ablation process was verified by a simple model to begin well below the MAVEN periapsis altitude, and therefore no correction of the dust flux as function of altitude is needed (5). Because of the agreement between the observed and predicted fluxes, and the nearly constant flux rate with altitude for low spacecraft potentials (Fig. 3), we conclude that MAVEN probably is observing interplanetary dust at Mars.

There are other indications that the dust observed by MAVEN is of interplanetary origin. During MAVEN's cruise phase, when the booms were stowed, the instrument detected dust particles in the interplanetary medium, although a direct flux comparison cannot be made because of the different instrument configuration. In addition, observations of dust above Mars are fairly constant up to $\sim 3000 \text{ km}$, suggesting a source far from the planet. Finally, interplanetary dust is expected to have a preferred flow direction with respect to the motion of the planet. The dust fluxes observed thus far as MAVEN's orbit precessed show no indication of being equatorially confined, whereas an increased flux on the day-side is observed (Fig. 2). The orbital coverage is currently too limited to conclusively indicate a favored directionality.

The dynamics of interplanetary dust influence atmospheric composition and planetary mass balances. Interplanetary dust contributes 0.6 to 30 kg s^{-1} to Earth's atmosphere (21). The surface area of Mars's atmosphere is smaller, and the speed of the dust particles should be $\sim 20\%$

Fig. 3. Fraction of data bursts containing a dust impact (hit), as function of altitude. The black dots encompass the full data set, whereas the red dots only show data bursts where the magnitude of the spacecraft potential was <3 V. The presented uncertainty is the standard deviation.

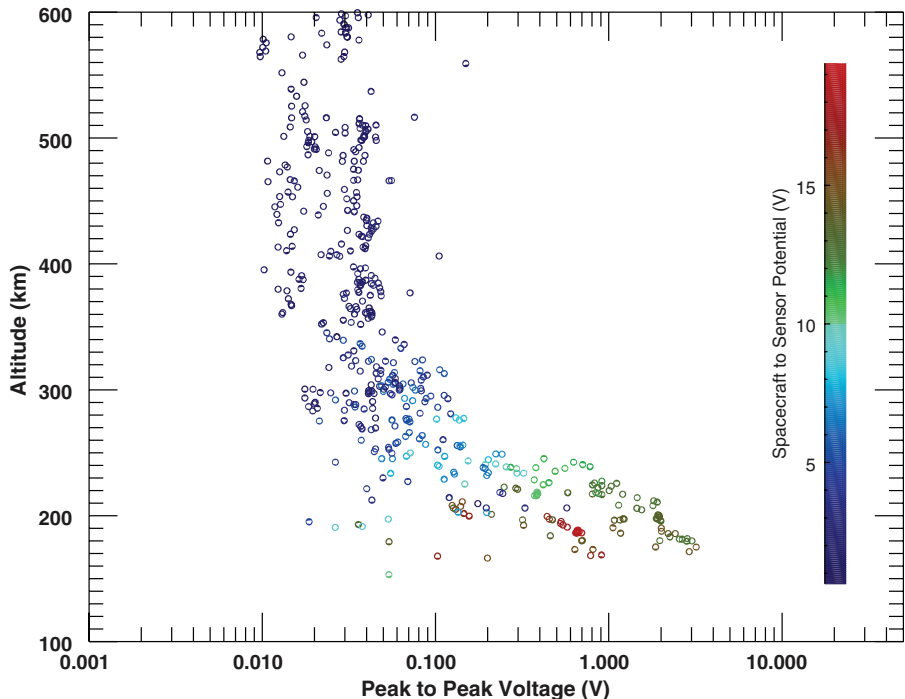
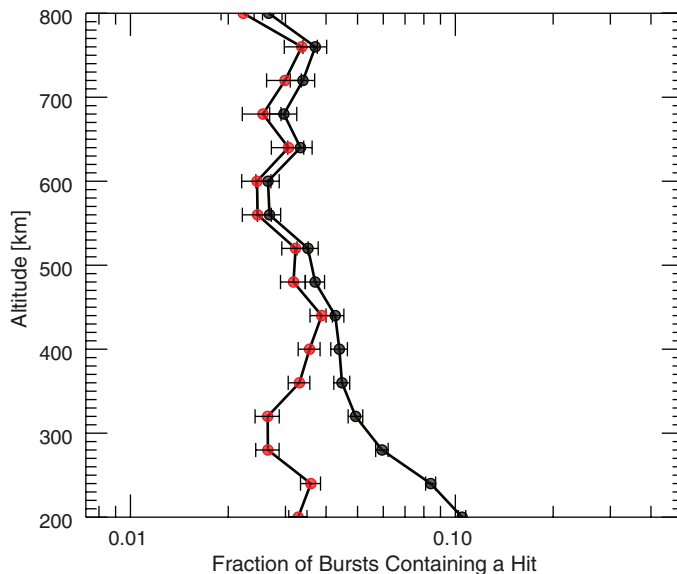


Fig. 4. Peak-to-peak amplitudes of dust impacts, as function of altitude. These observations were obtained when the LPW instrument measured the voltage between the sensor and the spacecraft. The spacecraft potential during the observed dust impact is indicated by the colors.

slower because of the increased distance from the Sun (21) and because interplanetary dust fluxes decrease farther out in the solar system (20). Based on these considerations, Mars's atmosphere would be expected to receive interplanetary dust at a rate of 0.1 to 3 kg s⁻¹. We estimate that the dust observed by MAVEN contributes only ~0.001 to 0.1 kg s⁻¹, based on observed fluxes (Fig. 2C) and the spacecraft velocity. Thus, we conclude that the observed dust particles

represent only a small portion of the likely total influx of interplanetary dust particles.

REFERENCES AND NOTES

1. S. A. Haider, V. Sheel, M. D. Smith, W. C. Maguire, G. J. Molina-Cuberos, Effect of dust storms on the D region of the Martian ionosphere: Atmospheric electricity. *J. Geophys. Res.* **115**, A12336 (2010). doi: [10.1029/2010JA016125](https://doi.org/10.1029/2010JA016125)
2. W.-H. Ip, M. Banaszekiewicz, On the dust/gas tori of Phobos and Deimos. *Geophys. Res. Lett.* **17**, 857–860 (1990). doi: [10.1029/GL017006p00857](https://doi.org/10.1029/GL017006p00857)

3. A. Zakharov, M. Horanyi, P. Lee, O. Witasse, F. Cipriani, Dust at the Martian moons and in the circummartian space. *Planet. Space Sci.* **102**, 171–175 (2014). doi: [10.1016/j.pss.2013.12.011](https://doi.org/10.1016/j.pss.2013.12.011)
4. V. N. Lebedinets, A. V. Manochina, V. B. Shushkova, Interaction of the lower thermosphere with the solid component of the interplanetary medium. *Planet. Space Sci.* **21**, 1317–1332 (1973). doi: [10.1016/0032-0633\(73\)90224-9](https://doi.org/10.1016/0032-0633(73)90224-9)
5. J. G. Molina-Cuberos, J. J. López-Moreno, F. Arnold, Meteoric layers in planetary atmospheres. *Space Sci. Rev.* **137**, 175–191 (2008). doi: [10.1007/s11214-008-9340-5](https://doi.org/10.1007/s11214-008-9340-5)
6. B. M. Jakosky et al., The Mars Atmosphere and Volatile Evolution (MAVEN) mission. *Space Sci. Rev.* **10.1007/s11214-015-0139-x** (2015).
7. L. Andersson et al., The Langmuir Probe and Waves (LPW) instrument for MAVEN. *Space Sci. Rev.* (2015). doi: [10.1007/s11214-015-0194-3](https://doi.org/10.1007/s11214-015-0194-3)
8. P. Oberc, Electric antenna as a dust detector. *Adv. Space Res.* **17**, 105–110 (1996). doi: [10.1016/0273-1177\(95\)00766-8](https://doi.org/10.1016/0273-1177(95)00766-8) pmid: [11540354](https://pubmed.ncbi.nlm.nih.gov/11540354/)
9. Materials and methods are available as supplementary materials on Science Online.
10. D. A. Gurnett, E. Grün, D. Gallagher, W. S. Kurth, F. L. Scarf, Micron-sized particles detected near Saturn by the Voyager plasma wave instrument. *Icarus* **53**, 236–254 (1983). doi: [10.1016/0019-1035\(83\)90145-8](https://doi.org/10.1016/0019-1035(83)90145-8)
11. P. Oberc, W. Parzydło, O. L. Vaisberg, Correlations between the Vega 2 plasma wave (APV-N) and dust (SP-1) observations at Comet Halley. *Icarus* **86**, 314–326 (1990).
12. B. T. Tsurutani et al., Dust impacts at Comet P/Borrelly. *Geophys. Res. Lett.* **30**, 2134 (2003). doi: [10.1029/2003GL017580](https://doi.org/10.1029/2003GL017580)
13. W. S. Kurth, T. F. Averkamp, D. A. Gurnett, Z. Wang, Cassini RPWS observations of dust in Saturn's E Ring. *Planet. Space Sci.* **54**, 988–998 (2006). doi: [10.1016/j.pss.2006.05.011](https://doi.org/10.1016/j.pss.2006.05.011)
14. A. Zaslavsky et al., Interplanetary dust detection by radio antennas: Mass calibration and fluxes measured by STEREO/WAVES. *J. Geophys. Res.* **117**, A05102 (2012). doi: [10.1029/2011JA017480](https://doi.org/10.1029/2011JA017480)
15. D. M. Malaspina et al., Interplanetary and interstellar dust observed by the Wind/WAVES electric field instrument. *Geophys. Res. Lett.* **41**, 266–272 (2014). doi: [10.1002/2013GL058786](https://doi.org/10.1002/2013GL058786)
16. A. Collette, G. Meyer, D. Malaspina, Z. Sternovsky, Laboratory investigation of antenna signals from dust impacts on spacecraft. *J. Geophys. Res. Space Phys.* **120**, 5298–5305 (2015). doi: [10.1002/2015JA021198](https://doi.org/10.1002/2015JA021198)
17. A. Collette, E. Grün, D. Malaspina, Z. Sternovsky, Micrometeoroid impact charge yield for common spacecraft materials. *J. Geophys. Res. Space Physics* **119**, 6019–6026 (2014). doi: [10.1002/2014JA020042](https://doi.org/10.1002/2014JA020042)
18. G. J. Molina-Cuberos, O. Witasse, J.-P. Lebreton, R. Rodrigo, J. J. López-Moreno, Meteoric ions in the atmosphere of Mars. *Planet. Space Sci.* **51**, 239–249 (2003). doi: [10.1016/S0032-0633\(02\)00197-6](https://doi.org/10.1016/S0032-0633(02)00197-6)
19. A. Sánchez-Lavega et al., An extremely high-altitude plume seen at Mars' morning terminator. *Nature* **518**, 525–528 (2015). doi: [10.1038/nature14162](https://doi.org/10.1038/nature14162); pmid: [25686601](https://pubmed.ncbi.nlm.nih.gov/25686601/)
20. E. Grün, A. n, H. Zook, R. H. Fechtig, Collisional balance of the meteoric complex. *Icarus* **62**, 244–272 (1985). doi: [10.1016/0019-1035\(85\)90121-6](https://doi.org/10.1016/0019-1035(85)90121-6)
21. I. Mann et al., Dusty plasma effects in near Earth space and interplanetary medium. *Space Sci. Rev.* **161**, 1–47 (2011). doi: [10.1007/s11214-011-9762-3](https://doi.org/10.1007/s11214-011-9762-3)

ACKNOWLEDGMENTS

The data used in our analyses are available via NASA's Planetary Data System at http://atmos.nmsu.edu/data_and_services/atmospheres_data/MAVEN/maven_main.html. NASA funding for the MAVEN project through the Mars Exploration Program supported this work.

SUPPLEMENTARY MATERIALS

www.sciencemag.org/content/350/6261/aad0398/suppl/DC1
Materials and Methods
Fig. S1

16 July 2015; accepted 17 September 2015
10.1126/science.aad0398

This copy is for your personal, non-commercial use only.

If you wish to distribute this article to others, you can order high-quality copies for your colleagues, clients, or customers by [clicking here](#).

Permission to republish or repurpose articles or portions of articles can be obtained by following the guidelines [here](#).

The following resources related to this article are available online at www.sciencemag.org (this information is current as of November 5, 2015):

Updated information and services, including high-resolution figures, can be found in the online version of this article at:

<http://www.sciencemag.org/content/350/6261/aad0398.full.html>

Supporting Online Material can be found at:

<http://www.sciencemag.org/content/suppl/2015/11/04/350.6261.aad0398.DC1.html>

A list of selected additional articles on the Science Web sites **related to this article** can be found at:

<http://www.sciencemag.org/content/350/6261/aad0398.full.html#related>

This article has been **cited by** 1 articles hosted by HighWire Press; see:

<http://www.sciencemag.org/content/350/6261/aad0398.full.html#related-urls>